

# The superconducting energy gap in the hole-doped graphene beyond the Migdal's theory

Adam Z. Kaczmarek<sup>1\*</sup> and Ewa A. Drzazga-Szcześniak<sup>2</sup>

<sup>1</sup>*Department of Theoretical Physics, Faculty of Science and Technology,  
Jan Długosz University in Częstochowa, 13/15 Armii Krajowej Ave., 42200 Częstochowa, Poland and*

<sup>2</sup>*Department of Physics, Faculty of Production Engineering and Materials Technology,  
Częstochowa University of Technology, 19 Armii Krajowej Ave., 42200 Częstochowa, Poland*

(Dated: August 16, 2022)

In this work we analyze impact of non-adiabatic effects on the superconducting energy gap in the hole-doped graphene. By using the Eliashberg formalism beyond the Migdal's theorem, we present that the non-adiabatic effects strongly influence the superconducting energy gap in the exemplary boron-doped graphene. In particular, the non-adiabatic effects, as represented by the first order vertex corrections to the electron-phonon interaction, supplement Coulomb depairing correlations and suppress the superconducting state. In summary, the obtained results confirm previous studies on superconductivity in two-dimensional materials and show that the corresponding superconducting phase may be notably affected by the non-adiabatic effects.

## I. INTRODUCTION

The discovery of graphene has led to the ever-growing interested in its electronic properties [1]. Among various electronic aspects, a notable attention was given to the induction of the conventional superconducting state in this material. In this respect, one the most promising scenarios were realized via doping graphene with a foreign atoms [2–5]. In general, there are two main routes to enhance graphene's electron-phonon coupling ( $\lambda$ ). First is the so-called surface functionalization, where metal atoms are deposited at the surface of the monolayer [2, 6, 7]. Unfortunately, in this approach, the resulting critical temperature of the superconductive state ( $T_C$ ) is rather low. However, the second strategy aims at the introduction of impurities which act like a electron or hole dopants and lead to the much higher  $T_C$  values [3, 4, 8].

Along with a relatively high  $T_C$  values of the substitutionally doped graphene, such material exhibits shallow conduction band [3, 4], similarly to fullerenes and fullerides [9–12]. This leads to the significant value of the phonon and electron energy scales ratio ( $\omega_D/E_F$ , where  $\omega_D$  is the Debye's frequency and  $E_F$  denotes Fermi energy), which cannot be neglected in the framework of the Migdal's theorem [13]. Such behavior results in the non-adiabatic effects strongly influencing the superconducting phase [14, 15]. As suggested in [14, 16], the non-adiabatic effects may have nontrivial impact on the electron-phonon interaction, that can be observed based on the order parameter behavior. For example, proper characterization of these effects in graphene was recently described for the electron-doped graphene structures in [8]. To be specific, the Authors of [8] have shown that the contribution of the non-adiabatic effects is rising upon the increase of the Coulomb interaction.

With respect to the above, we investigate the non-

adiabatic effects in case of the hole-doped graphene, to determine their impact on the order parameter and the  $T_C$  value. To do so, we employ the Eliashberg equations [17] with the first order vertex-corrections [11, 15, 18]. The calculations are done for the 50% boron-doped graphene structure ( $h$ -CB) under biaxial tensile strain  $\epsilon = 5\%$  and at the moderate level of the dopant electrons ( $n = -0.2|e|/\text{unit cell}$ ) [4].

## II. THEORETICAL MODEL

As already mentioned, the present analysis is based on the Eliashberg formalism [17, 19]. Conventionally this formalism is employed within the adiabatic regime *i.e.* by assuming the Migdal's theorem [13]. However, to analyze the non-adiabatic effect the Eliashberg equations are additionally generalized here by considering the first order vertex corrections to the electron-phonon interaction [14, 18, 20].

Specifically, we assume that the adiabatic Eliashberg equations on the imaginary axis have the form:

$$\phi_n = \pi k_B T \sum_{m=-M}^M \frac{[K_{n,m} - \mu^* \theta(\omega_c - |\omega_m|)]}{\sqrt{\omega_m^2 Z_m^2 + \phi_m^2}} \phi_m, \quad (1)$$

$$Z_n = 1 + \pi k_B T \sum_{m=-M}^M \frac{K_{n,m}}{\sqrt{\Delta_m^2 + \omega_m^2}} \frac{\omega_m}{\omega_n} Z_m. \quad (2)$$

where  $\phi_n = \phi(i\omega_n)$  denotes the order parameter function and  $Z_n = Z(i\omega_n)$  is the renormalization factor of the wave function. In what follows,  $k_B$  is the Boltzmann constant,  $T$  denotes the temperature, and  $\omega_n$  represents the  $n$ -th Matsubara frequency ( $\omega_n = \pi k_B T (2n + 1)$ ). In this framework,  $M$  denotes the cut-off value for the calculations and is equal to 1100, so the numerical calculations are stable for  $T > 5$  K. Moreover,  $\mu_n^* = \mu^* \theta(\omega_c - |\omega_n|)$  is the Coulomb pseudopotential which models the depairing

\*Electronic address: adam.kaczmarek@doktorant.ujd.edu.pl

correlations; where  $\theta$  is the Heaviside function and  $\omega_c$  represents the cut-off frequency.

In the above equations, the electron-phonon pairing kernel is expressed as:

$$K_{n,m} \equiv 2 \int_0^{\omega_D} d\omega \frac{\omega}{4\pi^2 k_B^2 T^2 (n-m)^2 + \omega^2} \alpha^2 F(\omega), \quad (3)$$

where  $\alpha^2 F(\omega)$  denotes the Eliashberg function for a given  $\omega$  phonon energy:

$$\alpha^2 F(\omega) = \frac{1}{2\pi\rho(E_F)} \sum_{\mathbf{q}\nu} \delta(\omega - \omega_{\mathbf{q}\nu}) \frac{\gamma_{\mathbf{q}\nu}}{\omega_{\mathbf{q}\nu}}, \quad (4)$$

whereas:

$$\gamma_{\mathbf{q}\nu} = 2\pi\omega_{\mathbf{q}\nu} \sum_{ij} \int \frac{d^3k}{\Omega_{BZ}} |g_{\mathbf{q}\nu}(\mathbf{k}, i, j)|^2 \times \delta(E_{\mathbf{q},i} - E_F) \delta(E_{\mathbf{k}+\mathbf{q},j} - E_F). \quad (5)$$

In Eq. (5), the  $\omega_{\mathbf{q}\nu}$  gives values of the phonon energies and  $\gamma_{\mathbf{q}\nu}$  denotes the phonon linewidth. In this context, the electron-phonon coefficients are represented by  $g_{\mathbf{q}\nu}(\mathbf{k}, i, j)$  and  $E_{\mathbf{k},i}$  stands for the electron band energy. Note that the higher order corrections are not included in Eq. (3), and that the momentum dependence of electron-phonon matrix elements has been neglected in Eq. (6) and Eq. (7) (in accordance to the local approximation). Therefore, the order parameter can be written as:  $\Delta_n(T, \mu^*) = \phi_n/Z_n$ . Finally, we note that for the purpose of our research, we use Eliashberg function given in [4]. It is important to remark, that the resulting cutoff frequency in Eq. (1) is  $\omega_C = 10\omega_{\max}$  with the maximum phonon frequency equal to  $\omega_{\max} = 124.47$  meV.

With respect to the presented adiabatic equations, the introduction of the first-order vertex correction terms leads to the non-adiabatic Eliashberg equations (N-E) of the following form [8, 20]:

$$\begin{aligned} \phi_n &= \pi k_B T \sum_{m=-M}^M \frac{K_{n,m} - \mu_m^*}{\sqrt{\omega_m^2 Z_m^2 + \phi_m^2}} \phi_m - \beta \frac{\pi^3 (k_B T)^2}{4E_F} \\ &\times \sum_{m=-M}^M \sum_{m'=-M}^M \frac{K_{n,m} K_{n,m'}}{\sqrt{(\omega_m^2 Z_m^2 + \phi_m^2) (\omega_{m'}^2 Z_{m'}^2 + \phi_{m'}^2) (\omega_{-n+m+m'}^2 Z_{-n+m+m'}^2 + \phi_{-n+m+m'}^2)}} \\ &\times (\phi_m \phi_{m'} \phi_{-n+m+m'} + 2\phi_m \omega_{m'} Z_{m'} \omega_{-n+m+m'} Z_{-n+m+m'} - \omega_m Z_m \omega_{m'} Z_{m'} \phi_{-n+m+m'}), \end{aligned} \quad (6)$$

and

$$\begin{aligned} Z_n &= 1 + \frac{\pi k_B T}{\omega_n} \sum_{m=-M}^M \frac{K_{n,m}}{\sqrt{\omega_m^2 Z_m^2 + \phi_m^2}} \omega_m Z_m - \beta \frac{\pi^3 (k_B T)^2}{4E_F \omega_n} \\ &\times \sum_{m=-M}^M \sum_{m'=-M}^M \frac{K_{n,m} K_{n,m'}}{\sqrt{(\omega_m^2 Z_m^2 + \phi_m^2) (\omega_{m'}^2 Z_{m'}^2 + \phi_{m'}^2) (\omega_{-n+m+m'}^2 Z_{-n+m+m'}^2 + \phi_{-n+m+m'}^2)}} \\ &\times (\omega_m Z_m \omega_{m'} Z_{m'} \omega_{-n+m+m'} Z_{-n+m+m'} + 2\omega_m Z_m \phi_{m'} \phi_{-n+m+m'} - \phi_m \phi_{m'} \omega_{-n+m+m'} Z_{-n+m+m'}). \end{aligned} \quad (7)$$

Note that when vertex-corrections contribution terms are neglected, the above Eliashberg equations take the adiabatic form of Eqs. (1) and (2).

### III. RESULTS AND DISCUSSION

We begin our discussion by noting that the adiabatic (A-E) and the non-adiabatic (N-E) equations presented in the previous section allows us to obtain the order parameter dependence on the temperature in the form:  $\Delta_n(T, \mu^*) = \frac{\phi_n}{Z_n}$ . This is done by using the numerical techniques presented originally in [20–22]. In such analysis, the special attention is paid to the maximum value of the

order parameter  $\Delta_{m=1}(T, \mu^*)$ , which equals to zero when  $T = T_C$  and  $\mu^* = \mu_C^*$ . In other words, it allows us to determine the critical value of the temperature for a given critical value of the Coulomb pseudopotential ( $\mu_C^*$ ), which is considered here as a free parameter. The latter one is assumed due to the fact that there are no experimental predictions of the  $T_C$  for the hole-doped graphene in the literature.

Specifically, our analysis is constrained to the three different values of  $\mu_C^*$ . In this way we can span relatively wide range of the  $\mu^*$  values, allowing for future comparisons with existing literature on the graphene-based superconductors [22–24] or with the experimental estimates. Fig. (1) depicts results of the numerical analysis for three different values of  $\mu^*$ . The adiabatic solutions are represented by purple symbols, while the gray ones

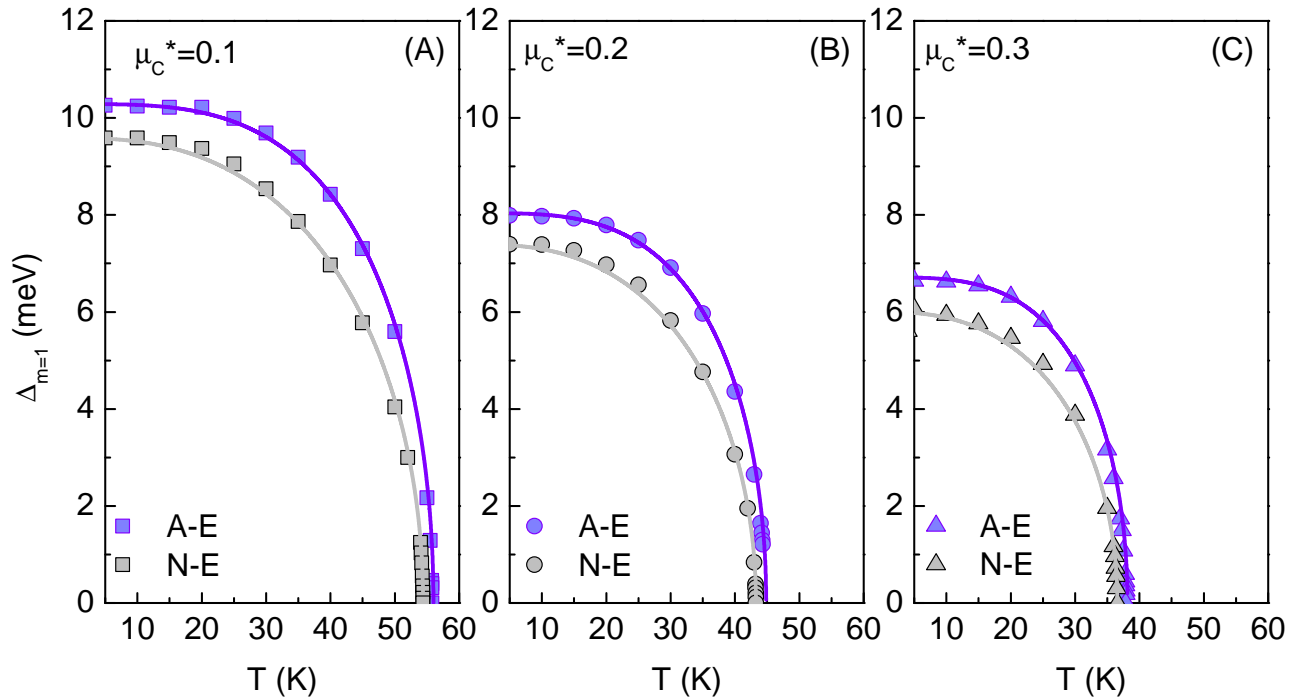


FIG. 1: The temperature dependence of the order parameter for selected  $\mu$  values. The adiabatic Eliashberg solutions are marked by the purple symbols whereas the non-adiabatic results by the gray ones. The solid lines are guide to an eye.

corresponds to the non-adiabatic Eliashberg equations associated with the vertex corrections. The presented results exhibits conventional behavior for the superconductors with the electron-phonon pairing mechanism, where  $\Delta_{m=1}$  has plateau at lower temperatures and decreases quickly for the higher ones.

However, the main observation can be made when comparing the adiabatic and non-adiabatic results. Namely, the inclusion of the vertex corrections in the theoretical framework leads to the decrease of the  $\Delta_{m=1}$  parameter for the entire range of  $T$  and  $\mu^*$ . The thermodynamic properties originated from this fact may be observed in the experiment. To be specific, lower  $\Delta_{m=1}$  for the non-adiabatic equations leads to  $T_C \in \langle 54.4, 36.6 \rangle$  K in comparison with the values obtained for the adiabatic scenario:  $T_C \in \langle 55.8, 37.9 \rangle$  K. Therefore, the non-adiabatic effects slightly lower critical temperature by  $\sim 1\%$ . We note that upon comparison with the electron-doped graphene [8], the decrease of the  $T_C$  is smaller. In fact, for the  $h$ -CN structure, changes are noticeable. To be specific, in the non-adiabatic framework the critical temperature is decreasing by  $\sim 30\%$ . Henceforth, the non-adiabatic effects in the hole-doped graphene are more favorable from the standpoint of keeping nominal  $T_C$  as high as possible. Influence of the non-adiabatic effects are another suppressor of the high  $T_C$  values besides the Coulomb pseudopotential. Implications of the non-adiabatic effects can also be seen at the origin of the temperature axis. In particular, the  $\Delta_{m=1}$  for  $T_0$ , which corresponds to the half-width of the superconducting gap ( $\Delta$ ), is also lower

for the non-adiabatic solutions than in the adiabatic case. Upon increase of the  $\mu^*$ ,  $\Delta \in \langle 10.3, 6.7 \rangle$  meV for the adiabatic case and  $\Delta \in \langle 9.6, 6.0 \rangle$  meV for the non-adiabatic case. Hence, the inclusion of the vertex corrections decrease the value of  $\Delta$  by  $\sim 5\%$  and  $\sim 10\%$ , respectively. By comparison with the twin  $h$ -CN material, the result of these corrections are significantly smaller [8]. In fact, the non-adiabatic effects in the electron-doped graphene are decreasing value of the order parameter by  $\sim 40\%$ .

From the perspective of the future experimental search, obtained values of the  $\Delta$  and  $T_C$  parameters may not be sufficient for the identification of the non-adiabatic effects in the hole-doped graphene. Thus, one should calculate characteristic ratio for the order parameter [19]:

$$R_\Delta \equiv 2\Delta(0)/k_B T_C. \quad (8)$$

The Eq. (8) originates from the BCS theory [25, 26] and as a dimensionless parameter it is important from the perspective of experiments conducted in the future. Here, by using Eq. (8) we obtain  $R_\Delta \in \langle 4.08, 3.79 \rangle$  and  $R_\Delta \in \langle 4.28, 4.09 \rangle$ . Again, the non-adiabatic effects lead to the reduction of the thermodynamic parameter value. It is important to note that for both types of the Eliashberg equations, values of parameter  $R_\Delta$  are higher than the standard BCS value of 3.53 [19, 25, 26]. Moreover, the difference between the non-adiabatic and adiabatic values of the characteristic ratio  $R_\Delta$  is much smaller than the ratio encountered in the case of its nitrogen-doped counterpart [8]. From the analysis presented above, one can also conclude that the retardation effects and strong

TABLE I: The thermodynamic quantities of the hole-doped graphene, as calculated in the present paper: the critical temperature  $T_C$ , the superconducting gap half-width ( $\Delta$ ) and the characteristic ratio  $R_\Delta$ . Results are obtained for the adiabatic (A-E) and non-adiabatic (N-E) Eliashberg approach.

$\mu^*$	$T_C$ (A-E) K	$T_C$ (N-E) K	$\Delta$ (A-E) meV	$\Delta$ (N-E) meV	$R_\Delta$ (A-E)	$R_\Delta$ (N-E)
0.1	55.8	54.4	10.3	9.6	4.27	4.08
0.2	44.1	43.1	8.1	7.3	4.16	3.96
0.3	37.9	36.6	6.7	6.0	4.09	3.79

coupling have an impact on the superconducting state in the hole-doped graphene.

#### IV. SUMMARY

We have tackled theoretical and numerical analysis within the Eliashberg theory to discuss possible impact of the non-adiabatic effects on the thermodynamic properties of the superconducting state in the hole-doped graphene ( $h$ -CB). Our analysis has been performed to analyze behavior of the critical temperature ( $T_C$ ), the superconducting gap half-width ( $\Delta$ ) and the dimensionless BCS-ratio for the order parameter ( $R_\Delta$ ). Values of these parameters for the adiabatic and non-adiabatic equations are summarized and presented in Table (I). Is it clear, that inclusion of the non-adiabatic effects, via vertex corrections to the electron-phonon interaction, reduces values of the thermodynamic parameters. It is also worth to

notice that for the stronger electron-coupling displayed by the higher  $\mu^*$  values, the non-adiabatic effects become slightly stronger. In other words, the Coulomb interaction is supplemented by the non-adiabatic effects. Moreover, these effects are significantly smaller than in the case of the electron-doped graphene analyzed in [8]. It means that the hole-doped graphene is more robust against the non-adiabatic effects, since these effects are decreasing its critical temperature ( $T_C$ ) minimally.

Finally, the results presented here supplement observations conducted for the electron-doped graphene structure [8]. In the comparison with the electron-doping, the hole-doped structure is more robust against the non-adiabatic effects [8]. However, the superconducting properties will still be decreased in the framework of the vertex-corrected Eliashberg equations. In general, the hole-doped graphene may be a still interesting choice for the phonon-induced superconducting material.

- 
- [1] A. H. Castro Neto, F. Guinea, N. M. R. Peres, K. S. Novoselov, and A. K. Geim, *Rev. Mod. Phys.* **81**, 109 (2009).
  - [2] G. Profeta, M. Calandra, and F. Mauri, *Nat. Phys.* **8**, 131 (2012).
  - [3] G. Savini, A. C. Ferrari, and F. Giustino, *Phys. Rev. Lett.* **105**, 037002 (2010).
  - [4] J. Zhou, Q. Sun, Q. Wang, and P. Jena, *Phys. Rev. B* **92**, 064505 (2015).
  - [5] R. Gholami, R. Moradian, S. Moradian, and W. E. Pickett, *Sci. Rep.* **8**, 13795 (2018).
  - [6] J. McChesney, A. Bostwick, T. Ohta, T. Seyller, K. Horn, J. González, and E. Rotenberg, *Phys. Rev. Lett.* **104**, 136803 (2010).
  - [7] J. Zhou, Q. Sun, Q. Wang, and P. Jena, *Phys. Rev. B* **90**, 205427 (2014).
  - [8] D. Szcześniak and E. A. Drzazga-Szcześniak, *EPL* **135**, 67002 (2021).
  - [9] M. P. M. Dean, C. A. Howard, S. S. Saxena, and M. Ellerby, *Phys. Rev. B* **81**, 045405 (2010).
  - [10] Y. Cao, V. Fatemi, S. Fang, K. Watanabe, T. Taniguchi, E. Kaxiras, and P. Jarillo-Herrero, *Nature* **556**, 43 (2018).
  - [11] L. Pietronero, *EPL* **17**, 365 (1992).
  - [12] O. Gunnarsson, *Rev. Mod. Phys.* **69**, 575 (1997).
  - [13] A. B. Migdal, *Sov. Phys. JETP* **34** (**7**), 996 (1958).
  - [14] L. Pietronero, S. Strässler, and C. Grimaldi, *Phys. Rev. B* **52**, 10516 (1995).
  - [15] C. Grimaldi, L. Pietronero, and S. Strässler, *Phys. Rev. B* **52**, 10530 (1995).
  - [16] L. Pietronero and E. Cappelluti, *Low Temp. Phys.* **32**, 340 (2006).
  - [17] G. M. Eliashberg, *Sov. Phys. JETP* **11**, 696 (1960).
  - [18] L. Pietronero and S. Strässler, *EPL* **18**, 627 (1992).
  - [19] J. P. Carbotte, *Rev. Mod. Phys.* **62**, 1027 (1990).
  - [20] J. K. Freericks, E. J. Nicol, A. Y. Liu, and A. A. Quong, *Phys. Rev. B* **55**, 11651 (1997).
  - [21] R. Szcześniak, *Acta Phys. Polon. A* **109**, 179 (2006).
  - [22] D. Szcześniak and R. Szcześniak, *Phys. Rev. B* **99**, 224512 (2019).
  - [23] R. Szcześniak and A. Barasiński, *Acta Phys. Polon. A* **116**, 1053–1058 (2009).
  - [24] R. Szcześniak, E. A. Drzazga, and D. Szcześniak, *Eur. Phys. J. B* **88**, 52 (2015).
  - [25] J. Bardeen, L. N. Cooper, and J. R. Schrieffer, *Phys. Rev.* **106**, 162 (1957).
  - [26] J. Bardeen, L. N. Cooper, and J. R. Schrieffer, *Phys. Rev.* **108**, 1175 (1957).